Cationic Amines

Á. Kozma, G. Gopakumar, C. Farès, W. Thiel, M. Alcarazo*

Synthesis and Structure of Carbene-Stabilized N-Centered Cations $[L_2N]^+$, $[L_2NR]^{2+}$, $[LNR_3]^{2+}$, and $[L_3N]^{3+}$

Crystallized! Mono-, di-, and tricationic amines that display unprecedented chemical environments around the central nitrogen atom have been structurally characterized. Cyclic voltammetry experiments and density functional calculations have been performed to gain insight into the electronic structure of these new compounds.

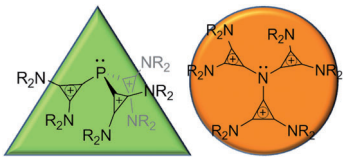

Chem. Eur. J.
DOI: **10.1002/chem.201204186**

Mesoporous Materials

Y. Yang, J. Liu, S. Bai, X. Li, Q. Yang*

Engineering the Mesopores of Fe_3O_4@Mesosilica Core–Shell Nanospheres through a Solvothermal Post-Treatment Method

Ghost in the shell: Fe_3O_4@mesosilica CSNs with a well-preserved morphology, mesoporous structure, and tunable large pore diameters (2.5–17.6 nm) were prepared through a new solvothermal post-treatment method. The resultant Fe_3O_4@mesosilica CSNs showed a higher adsorption capacity for benzene (up to 1.5 $g\,g^{-1}$) and lysozyme than that without pore expansion, thus making them a good candidate for loading large molecules.

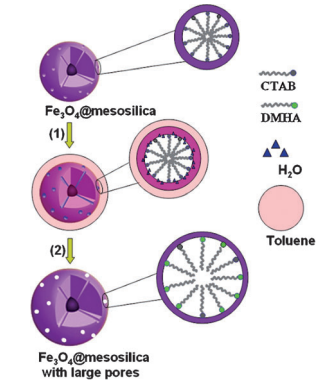

Chem. Asian J.
DOI: **10.1002/asia.201201026**

Terpenoids

N. L. Brock, K. Huss, B. Tudzynski,* J. S. Dickschat*

Genetic Dissection of Sesquiterpene Biosynthesis by *Fusarium fujikuroi*

A treasure trove of terpenes: The products of two fungal sesquiterpene synthases from the rice pathogen *Fusarium fujikuroi* were identified by gene-knockout experiments, genetic engineering of the fungus for production optimization, isolation of the sesquiterpenes, and structure elucidation by spectroscopic methods.

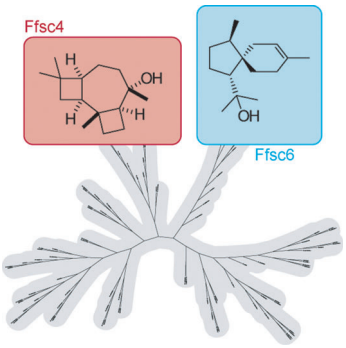

ChemBioChem
DOI: **10.1002/cbic.201200695**

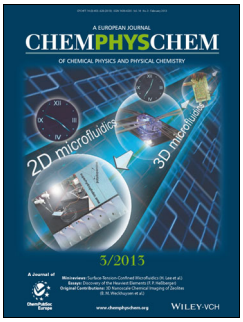

Photoluminescence

A. I. Chizhik,* I. Gregor, B. Ernst, J. Enderlein*

Nanocavity-Based Determination of Absolute Values of Photoluminescence Quantum Yields

In a new light: A new method for determining absolute values of quantum yield of luminescent emitters, based on the modification of the radiative transition of emitters within a tunable metallic nanocavity is presented. The method is easy to set up and works without any calibration. It will thus be useful for all applications where absolute and calibration-free measurements of luminescence quantum yields are needed.

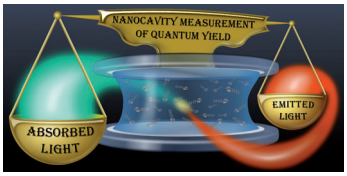

ChemPhysChem
DOI: **10.1002/cphc.201200931**

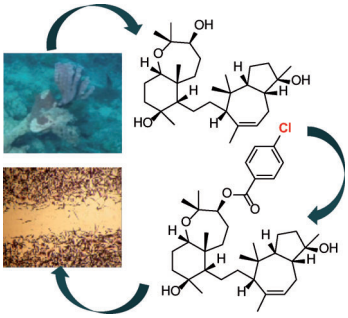

Marine Natural Products

A. I. Foudah, S. Jain, B. A. Busnena, K. A. El Sayed*

Optimization of Marine Triterpene Sipholenols as Inhibitors of Breast Cancer Migration and Invasion

Sipholenol A, a sipholane triterpene from *Callyspongia siphonella*, and its analogues are shown to have antimigratory activity in metastatic human breast cancer cells, while exhibiting no cytotoxicity towards normal epithelial cells. Evaluation of 19,20-anhydrosipholenol A 4β-benzoate ester against 451 human protein kinases identified protein tyrosine kinase 6 as a potential target. Sipholane triterpenoids represent novel antimigratory marine natural products with potential for development against metastatic malignancies.

ChemMedChem
DOI: **10.1002/cmdc.201200516**

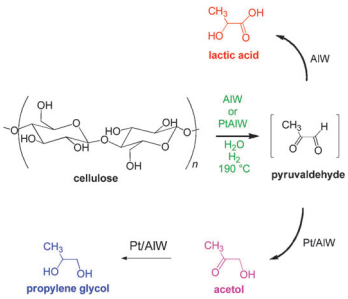

Renewables

F. Chambon, F. Rataboul,* C. Pinel, A. Cabiac, E. Guillon, N. Essayem

Cellulose Conversion with Tungstated-Alumina-Based Catalysts: Influence of the Presence of Platinum and Mechanistic Studies

Support for platinum: The hydrothermal treatment of cellulose under H_2 in the presence of tungstated alumina-based catalysts (AlW) yields lactic acid or acetol and propylene glycol as the main products depending on the presence or absence of supported platinum.

ChemSusChem
DOI: **10.1002/cssc.201200880**

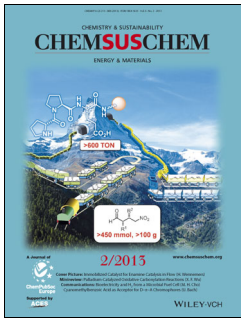

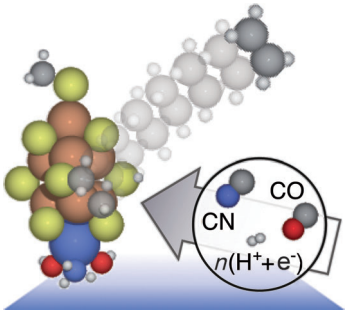

Fischer–Tropsch Processes

J. B. Varley, J. K. Nørskov*

First-Principles Calculations of Fischer–Tropsch Processes Catalyzed by Nitrogenase Enzymes

C–C coupling: The free energies of the CO and CN^- reduction pathways are calculated to identify the routes favored by FeMoco and FeVco nitrogenase active sites. The potential-limiting step in CO reduction is the initial protonation and adsorption of CHO*. CN^- reduction is limited by a second protonation of HCN. Higher-order hydrocarbons, limited by the same steps, are likely built from CH_2* intermediates common to both CO and CN^- reduction pathways.

ChemCatChem
DOI: **10.1002/cctc.201200635**

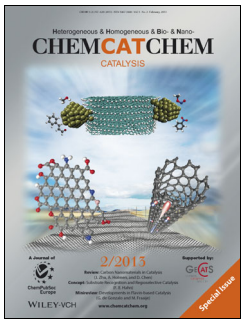

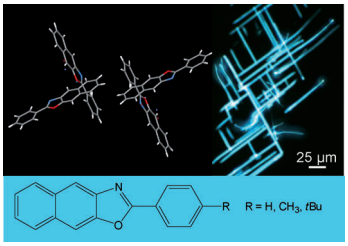

Dyes and Pigments

A. Ghodbane, J. Colléaux, N. Saffon, R. Mahiou, J.-P. Galaup, S. Fery-Forgues*

Blue-Emitting Nanocrystals, Microcrystals, and Highly Oriented Nanofibers Prepared by Reprecipitation and Solvent Drop-Casting of 2-Phenyl-naphthoxazoles

True blue: 2-Phenyl-naphthoxazole derivatives efficiently emit in the blue region (see figure) as a result of a favorable crystal packing mode. They readily gave micro/nanocrystals by using a solvent-exchange method. By solvent drop-casting, the unsubstituted derivative spontaneously generated highly oriented nanofibers. These compounds are promising candidates for the fabrication of blue-emitting tracers and nanofibers.

ChemPlusChem
DOI: **10.1002/cplu.201200233**

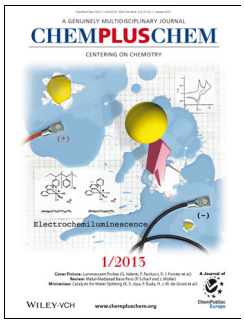

Spin Crossover

A. Grosjean, P. Négrier, P. Bordet, C. Etrillard, D. Mondieig, S. Pechev, E. Lebraud, J.-F. Létard, P. Guionneau*

Crystal Structures and Spin Crossover in the Polymeric Material $[Fe(Htrz)_2(trz)](BF_4)$ Including Coherent-Domain Size Reduction Effects

The crystal packing of the polymeric spin-crossover material $[Fe(Htrz)_2(trz)](BF_4)$ shows short N–H···N, between polymer chains, which is revealed by the positioning of the Htrz (1*H*-1,2,4-triazole) and trz^- ligands. Beyond the classical XRD study, a pair-distribution-function investigation shows that the crystal structure remains identical when the coherent-domain size is reduced to approximately 10 nm.

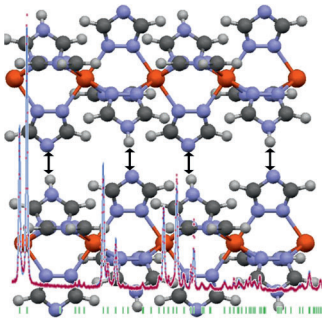

Eur. J. Inorg. Chem.
DOI: **10.1002/ejic.201201121**

Helical Structures

F. Kayamori, H. Abe,* M. Inouye*

Stabilization of Chiral Helices for Saccharide-Linked Ethynylpyridine Oligomers Possessing a Conformationally Well-Defined Linkage

etrameric and octameric 2,6-pyridylene ethynylene oligomers joined to a β-D-glucopyranoside by a *o*-phenylene linker were prepared and their higher-order structure studied. The chiral helical structures formed by intramolecular H-bonding and linker stabilization improve CD activity and resistance to protic surroundings. Stabilization was enhanced with the addition of $Cu(OTf)_2$ and $Zn(NO_3)_2$ salts.

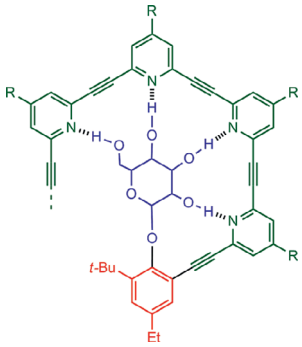

Eur. J. Org. Chem.
DOI: **10.1002/ejoc.201201376**

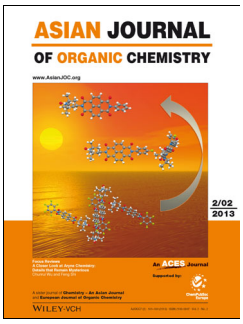

Synthetic Methods

A. Janiga, E. Glodkowska-Mrowka, T. Stoklosa, D. T. Gryko*

Synthesis and Optical Properties of Tetraaryl-1,4-dihydropyrrolo-[3,2-*b*]pyrroles

Hit for six! Six bonds are formed in a tandem process that gives rise to substituted 1,4-dihydropyrrole[3,2-*b*]pyrroles. Unparalleled simplicity and versatility of this one-pot reaction, no chromatography, as well as highly interesting optical properties have the potential to bring these molecules to the forefront in various applications.

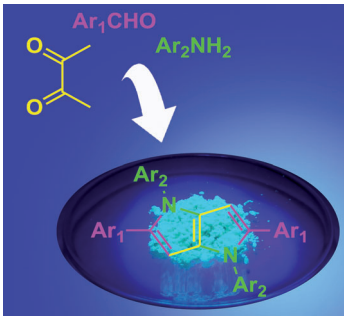

Asian J. Org. Chem.
DOI: **10.1002/ajoc.201200201**

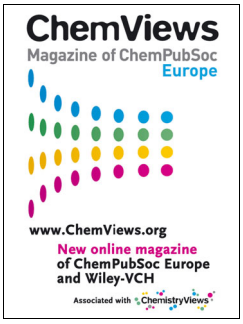

Food Chemistry

Klaus Roth

Our Daily Bread – Part 1

Chemistry plays an important role in every loaf of bread, from the grain, through its milling and grinding into flour to the final product. A truly unique bread paradise is Germany, with its host of numerous regional bread specialties. Klaus Roth, Berlin, Germany, starts in the first of three parts to reveal the secrets involved in transforming ripe ears of grain into a fragrant, aromatic bread.

ChemViews magazine
DOI: **10.1002/chemv.201300016**